Supplemetary Materials for Stress Drop Variations in the Region of the 2014 M_W8.1 Iquique Earthquake, Northern Chile

J. Folesky[1], J. Kummerow[1], S.A. Shapiro[1]
[1] Freie Universität Berlin, Department of Geophysics, Berlin, Germany
Corresponding author: jonas.folesky[at]geophysik.fu-berlin.de

February 23, 2021

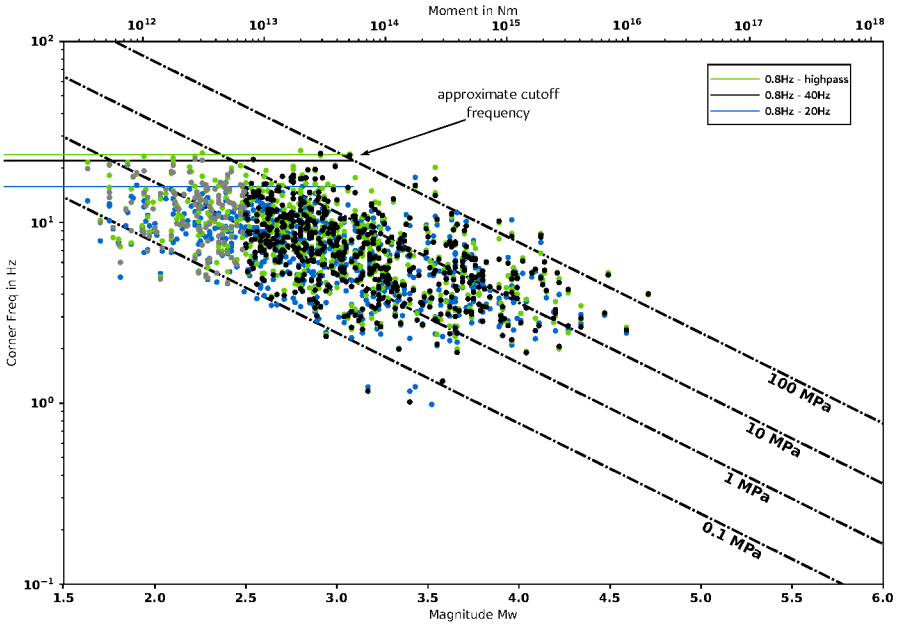

Figure S 1: Different bandpass filters lead to different cutoff frequencies which impact the estimated corner frequency value and thus influence the resulting stress drop estimates. We test three filters 1.) 0.8Hz highpass, 2.) 0.8-40Hz bandpass, and 3.) 0.8-20Hz bandpass. The figure shows the apparent cut-off frequencies for each filter. It also shows the shift of individual f_c values introduced by the filter choice. Based on this figure we chose the 0.8-40Hz bandpass filter and limit the corner frequency estimates that are interpreted in this paper to events with M>2.5.

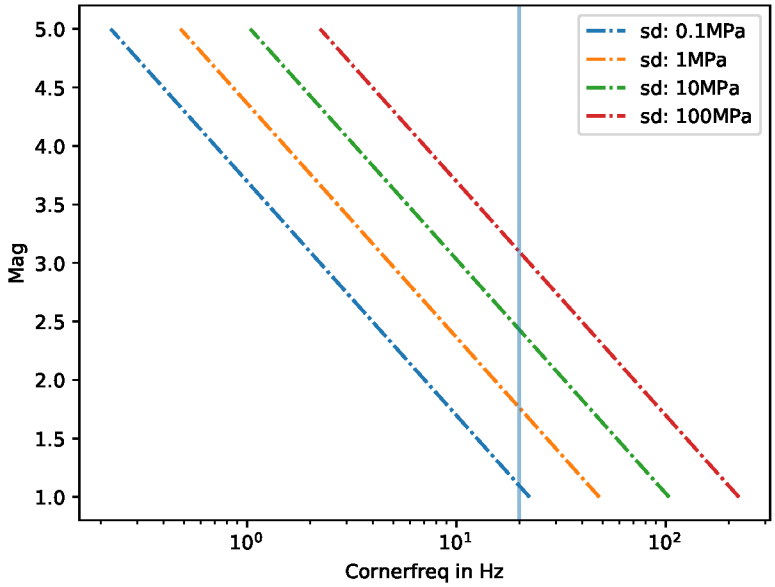

Figure S 2: Isolines of constant stress drop for different magnitudes and expected corner frequencies. The figure was computed based on Equation 4 in the manuscript. The input parameters are k=0.32 and vs=3900m/s. The vertical line is drawn at 20Hz which is half the upper bandpass filter corner (40Hz). Following this plot, the corner frequencies for all events with magnitudes M>2.5 are expected to be resolvable. Only high stress drop event (sd>10 MPa) in the range 2.5< M <3 will be affected by the upper cuttoff limit. We therefore exclude such events where $f_c > 20\,Hz$ (cf. Figure 11 main manuscript) Deselecting these events, however, appears to have an impact on the estimated scaling relation as discussed in the Results and Discussion section.

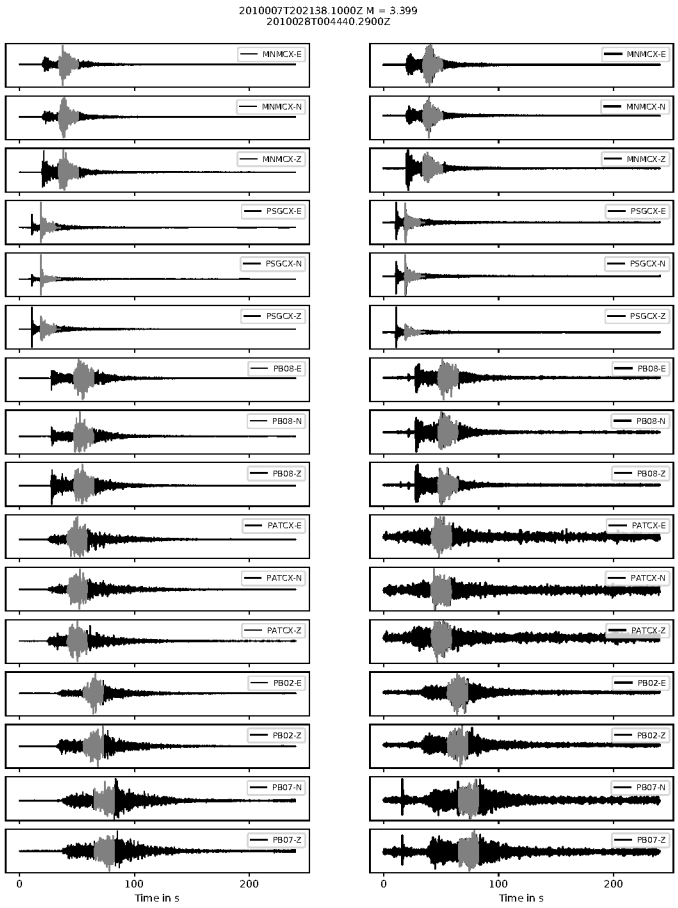

Figure S 3: Selected S phase windows for the same event as shown in Figures 3,4 & 5 from the main manuscript. On the left, the target event is shown; on the right, the EGF partner with the smaller magnitude. The utilized time windows are highlighted in grey.

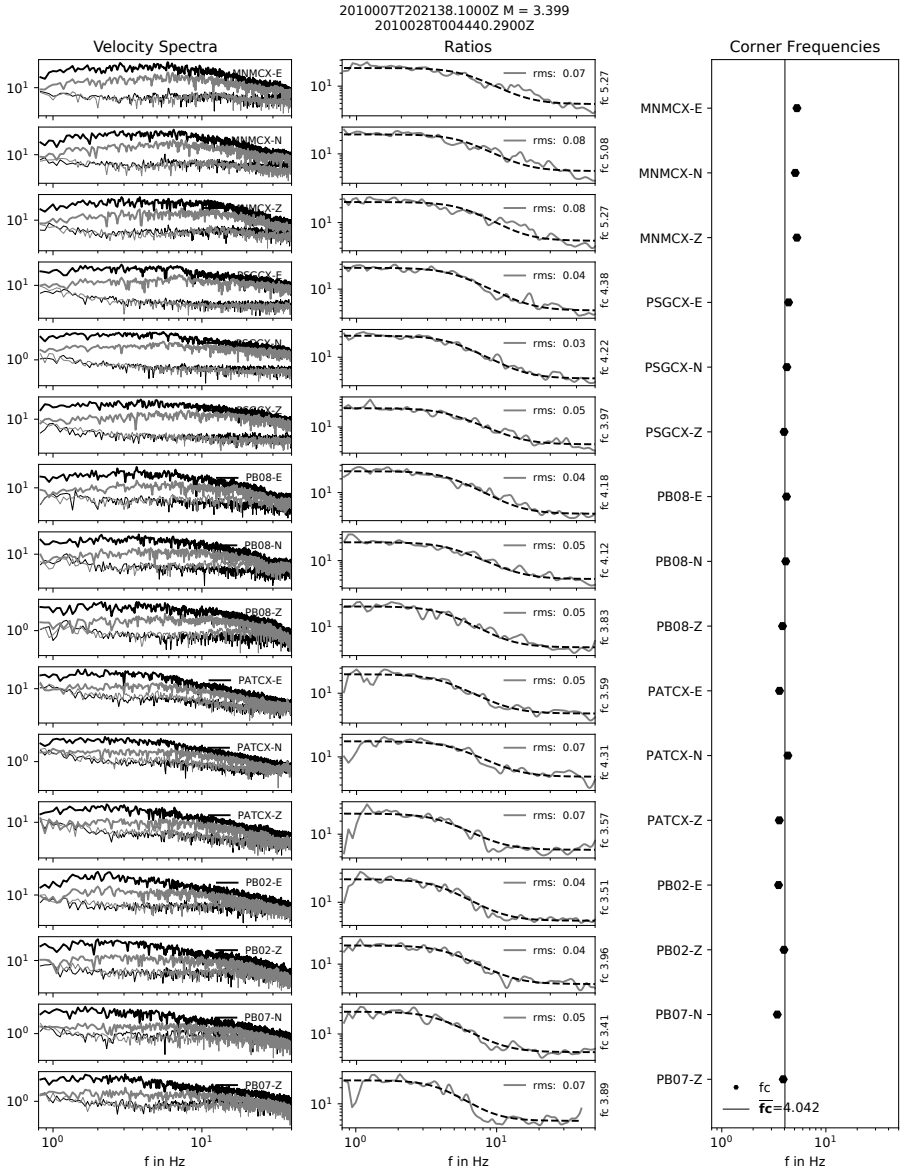

Figure S 4: Left: S phase velocity spectra of the event pair shown in Figure S 3 and corresponding noise spectra. Center: The spectral ratio and the Boatwright spectral model fit. Right: Station-wise corner frequencies with median value. Station sorting is north to south. A corner frequency of 4.0 Hz is estimated.

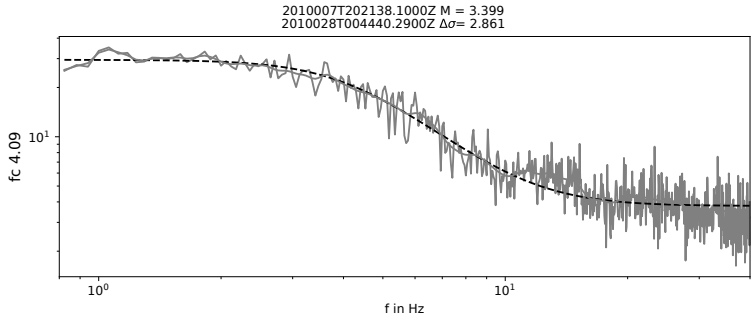

Figure S 5: Average velocity spectrum of S phase based spectra (Figure S 4). The stress drop value in the figure is preliminary. The correction is made after learning the k-ratio from Figure 2 main manuscript. The given value has to be corrected with a factor of 0.8 which yields a stress drop of $\Delta\sigma = 2.3\,\mathrm{MPa}$.

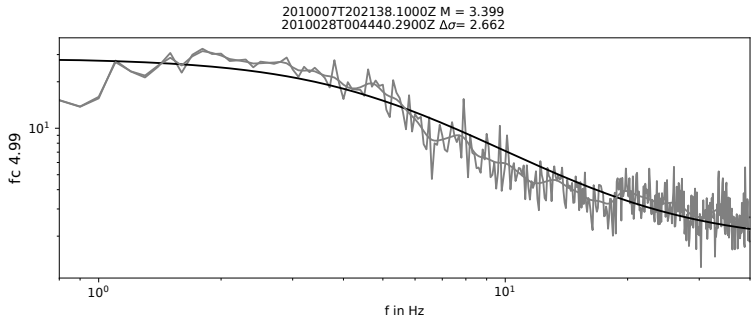

Figure S 6: Average velocity spectrum of P phase based spectra similar figure to Figure 5 from the main manuscript. Here, in contrast, the Brune type spectral model was used for fitting. Note that the characteristic shape of the spectrum is poorer described by the Brune type curve shape. This is the case for the great majority of events in our data set. We therefore decided to base our analysis on fitting the Boatwright model in order to obtain the corner frequencies.

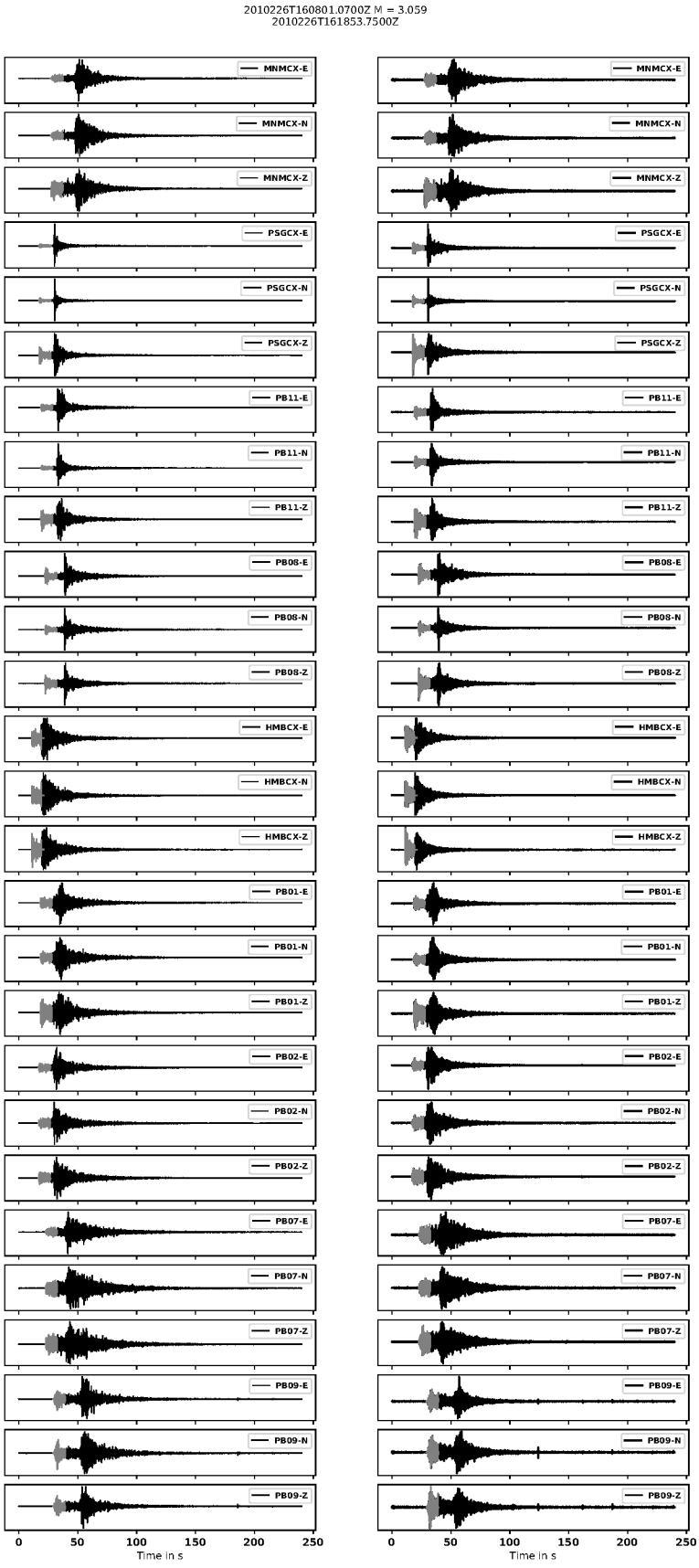

Figure S 7: P phase velocity traces for another main and EGF event.

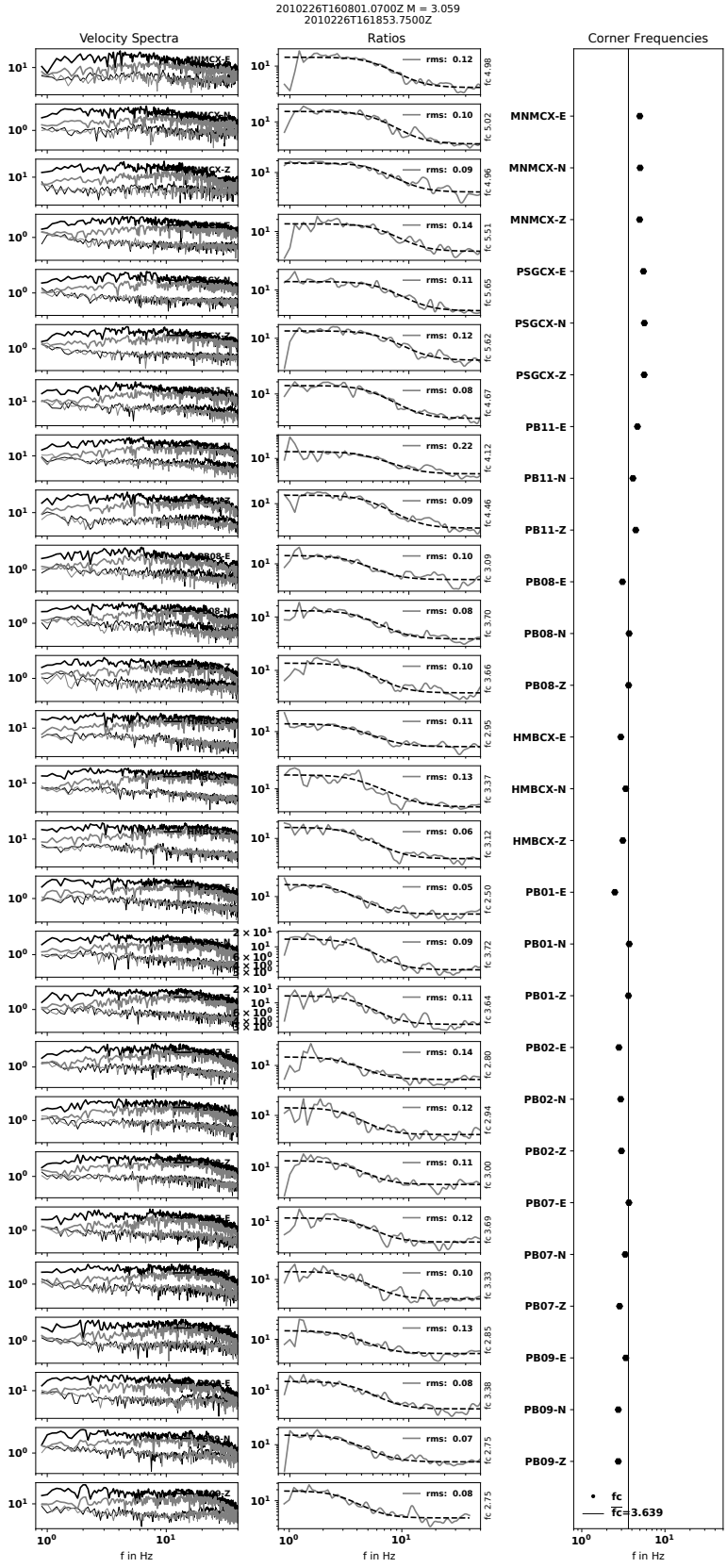

Figure S 8: Velocity spectra, spectral ratios and estimated corner frequencies.

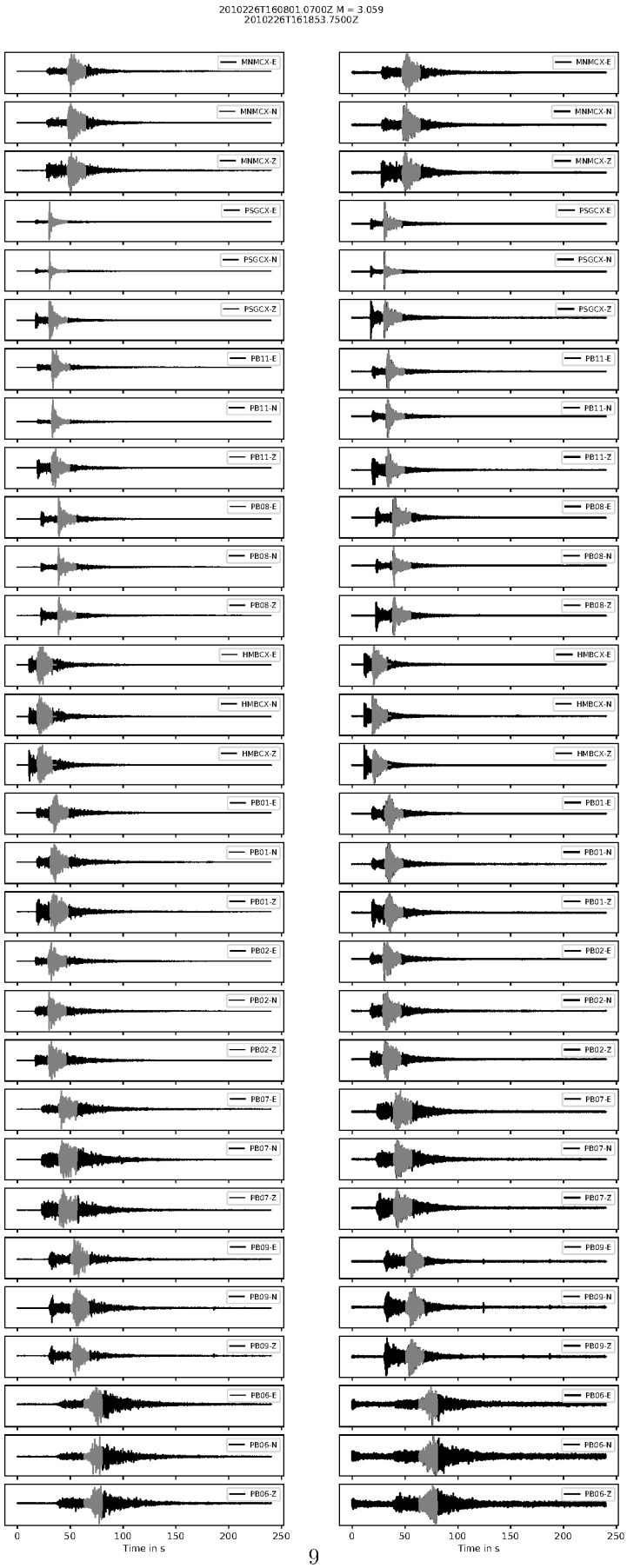

Figure S 9: Same as Figure S 7 but for S phase.

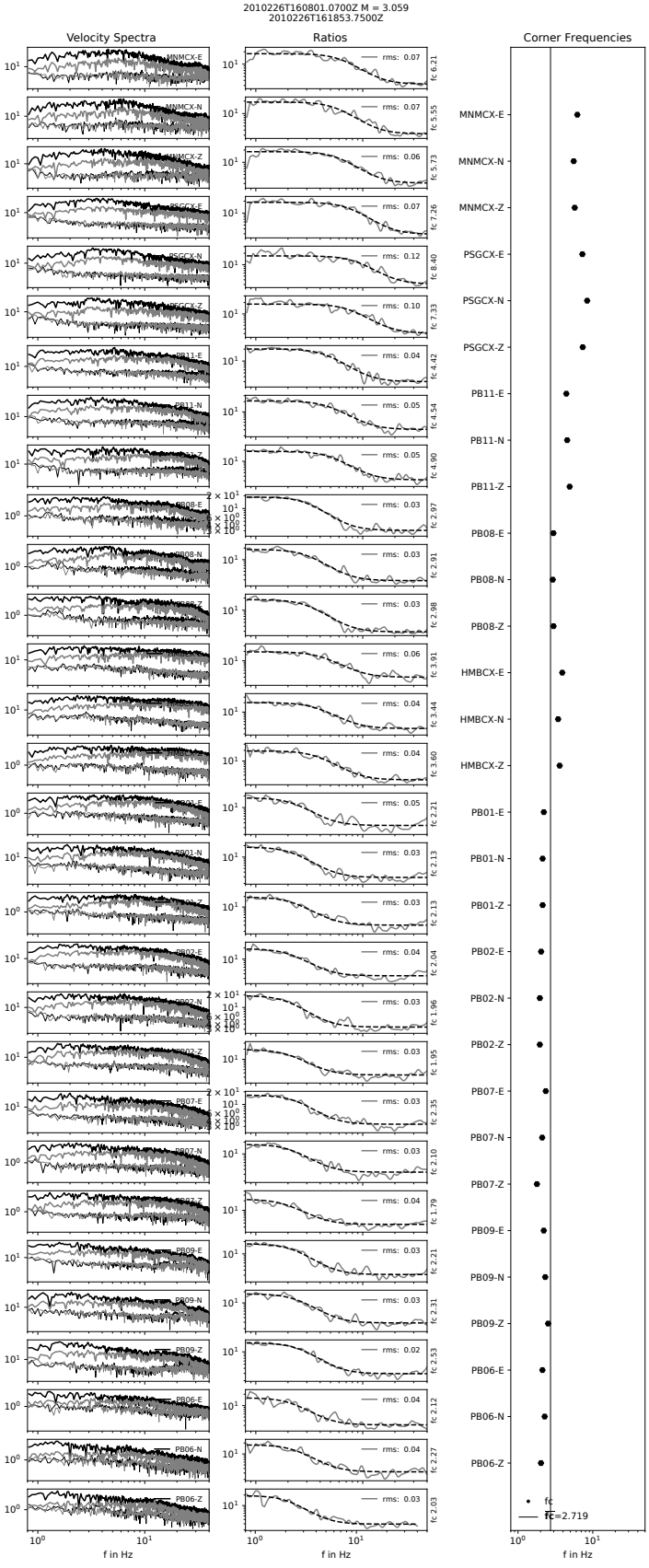

Figure S 10: Same as Figure S 8 but for S phase.

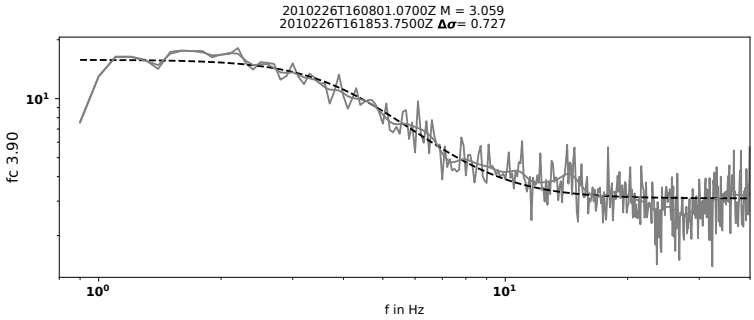

Figure S 11: Average spectral ratio for the traces shown in Figure S 8 and corresponding fit with corner frequency and stress drop estimate.

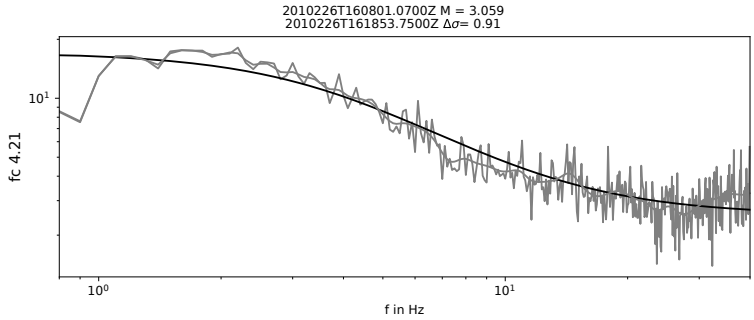

Figure S 12: Average spectral ratio as in Figure S 11 but fit with Brune spectral model. The curve shape does not fit as well a as the Boatwright model.

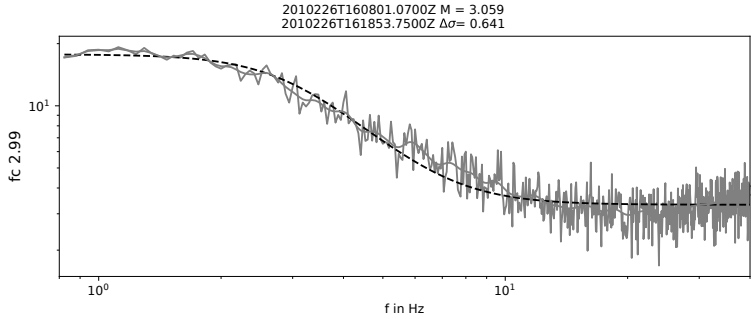

Figure S 13: Same as Figure S 11 for S phase. As explained above the stress drop has to be corrected with a factor of 0.8, yielding $\Delta\sigma = 0.51$.